Science Advances

AAAS

advances.sciencemag.org/cgi/content/full/3/12/eaar3952/DC1

Supplementary Materials for

In vivo genome editing improves motor function and extends survival in a mouse model of ALS

Thomas Gaj, David S. Ojala, Freja K. Ekman, Leah C. Byrne, Prajit Limsirichai, David V. Schaffer

Published 20 December 2017, *Sci. Adv.* **3**, eaar3952 (2017)
DOI: 10.1126/sciadv.aar3952

This PDF file includes:

- fig. S14. Mutant SOD1 inclusion bodies were visible in end-stage spinal cord sections from CRISPR-treated G93A-SOD1 mice.
- table S1. Oligonucleotides used in this study.
- table S2. External primers for MiSeq analysis.
- table S3. Internal primers for MiSeq analysis.

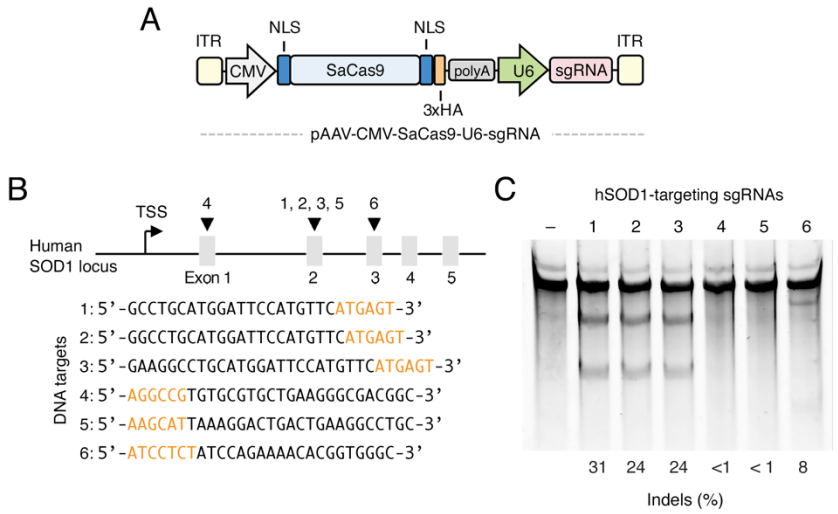

fig. S1. Designing sgRNA to target the human SOD1 gene. (A) AAV vector schematic. Abbreviations are as follows: ITR, inverted terminal repeat; CMV, cytomegalovirus promoter; NLS, nuclear localization signal sequence; 3xHA, three tandem repeats of the human influenza hemagglutinin (HA) epitope tag. **(B)** Schematic representation of the human SOD1 locus and candidate SaCas9 cleavage sites. Arrowheads indicate the exon in which each sgRNA target site is located. Orange bases denote protospacer-adjacent motif (PAM). **(C)** Frequency of hSOD1^{G93A} modification in neuroblastoma-spinal cord (NSC)-34-G93A-SOD1 cells transiently transfected with pAAV-CMV-SaCas9-U6-sgRNA-1-to-6. "-" indicates negative control. Indel frequencies were determined by the Surveyor nuclease assay. sgRNA-1 was used for *in vivo* studies.

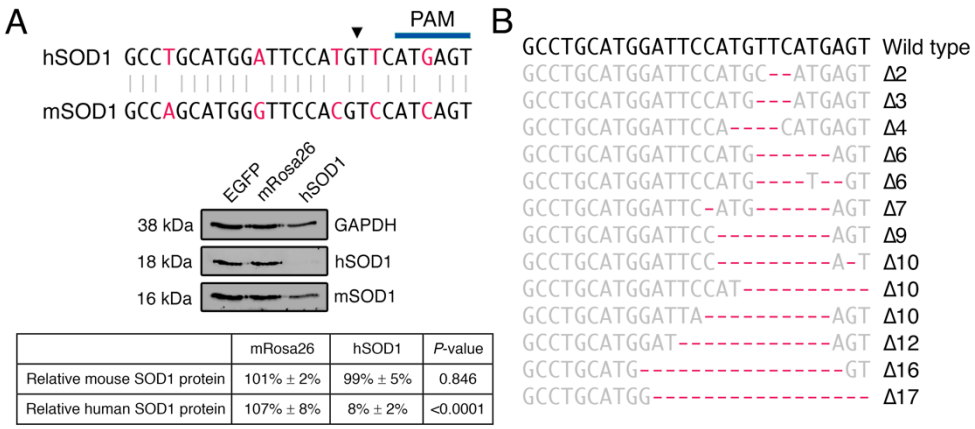

	mRosa26	hSOD1	*P*-value
Relative mouse SOD1 protein	101% ± 2%	99% ± 5%	0.846
Relative human SOD1 protein	107% ± 8%	8% ± 2%	<0.0001

fig. S2. CRISPR-Cas9 reduced mutant SOD1 expression in NSC-34–G93A–SOD1 cells by genome editing. (A, top) Alignment between the human and mouse SOD1 genes at the sgRNA target site. Nucleotide mismatches are colored pink. Arrowhead indicates the predicted SaCas9 cleavage site. **(A, middle)** Western blot of NSC-34-G93A-SOD1 lysate 72 h after transient transfection with pAAV plasmid encoding EGFP or SaCas9 with sgRNA targeting either the hSOD1 gene or the mouse Rosa26 locus. Transfected cells were enriched by FACS using a co-transfected surrogate reporter plasmid. **(A, bottom)** Quantitation of western blot results. Mouse and human SOD1 protein in cells transfected with SaCas9 and sgRNA targeting the hSOD1 gene or mRosa26 locus were normalized to GAPDH protein in each lane, and then compared to the same ratios in cells transfected with EGFP. Values are means of three independent replicates, and the error represents S.D. *P*-values were calculated using a two-way t-test. **(B)** Sanger sequencing of individual hSOD1^{G93A} transgenes cloned into pcDNA 3.1(+) from NSC-34-G93A-SOD1 cells transfected with pAAV-SaCas9-hSOD1. Indels are colored pink.

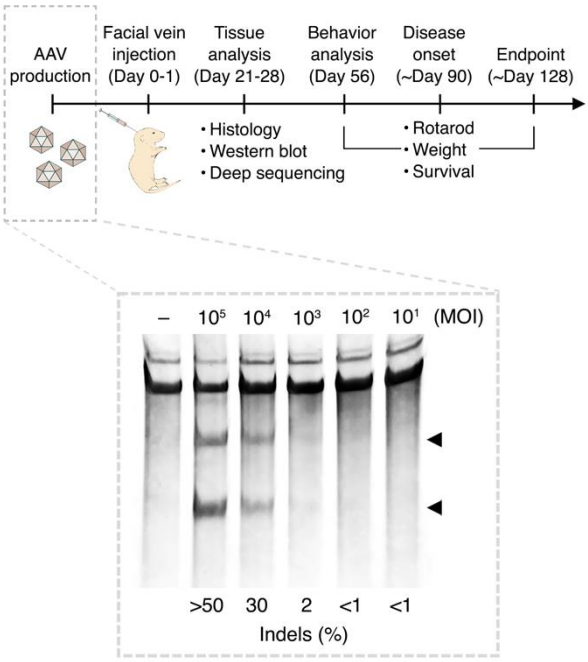

fig. S3. Quality control of AAV vectors. (Top) Experimental timeline for in vivo studies. AAV9 vectors encoding CRISPR-Cas9 were evaluated for their ability to modify hSOD1^{G93A} in cell culture prior to being administered to G93A-SOD1 mice. Inset shows the modification frequency of hSOD1^{G93A} cDNA in NSC-34-G93A-SOD1 cells infected with various multiplicities of infections (MOIs) of AAV9-SaCas9-hSOD1. Indel frequencies were determined by the Surveyor nuclease assay. "-" indicates negative control. Arrowheads indicate positions of the expected cleavage products.

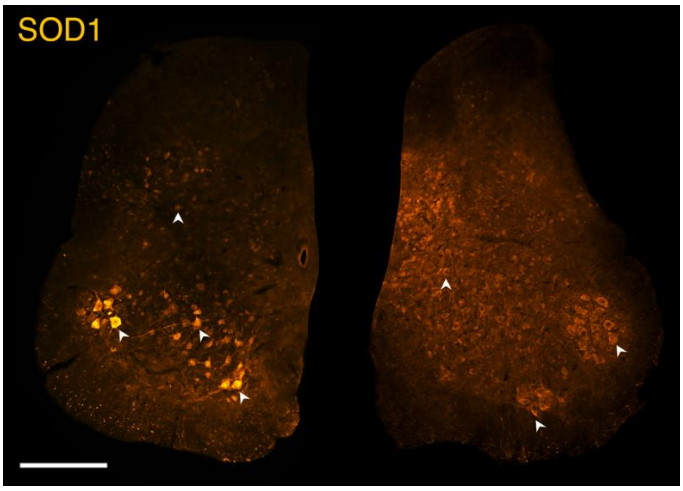

fig. S4. Mutant SOD1 expression in the spinal cord of untreated G93A-SOD1 mice. Immunofluorescent staining of representative lumbar (left) and thoracic (right) spinal cord hemisections from untreated P28 G93A-SOD1 mice. Arrowheads point to representative $SOD1^{+}$ cells. Scale bar, 200 μm.

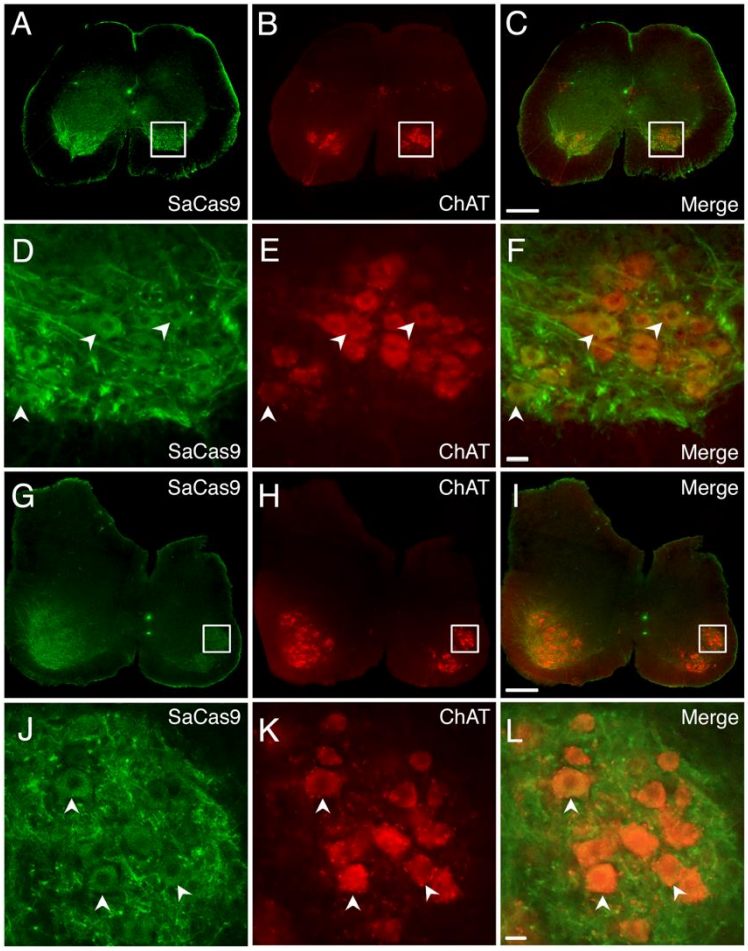

fig. S5. Systemic administration of AAV9-SaCas9-hSOD1 to neonatal G93A-SOD1 mice leads to SaCas9 expression in ChAT$^+$ cells in the spinal cord. (A-L) Immunofluorescent staining of **(A-F)** thoracic and **(G-L)** lumbar spinal cord sections four weeks after G93A-SOD1 mice were injected with AAV9-SaCas9-hSOD1 (n = 3) or AAV9-SaCas9-mRosa26 (n = 3) via facial vein at P0-P1. Insets show high magnification images from **(D-F)** thoracic and **(J-L)** lumbar spinal cord sections. Arrowheads point to representative SaCas9$^+$ and ChAT$^+$ cells. SaCas9 expression was observed in ~74% of examined ChAT$^+$ cells (n = 659, 568 and 872 ChAT$^+$ cells in lumbar, thoracic and cervical spinal cord sections, respectively) from three different mice. Scale bars, **(C, I)** 200 μm, **(F, L)** 20 μm.

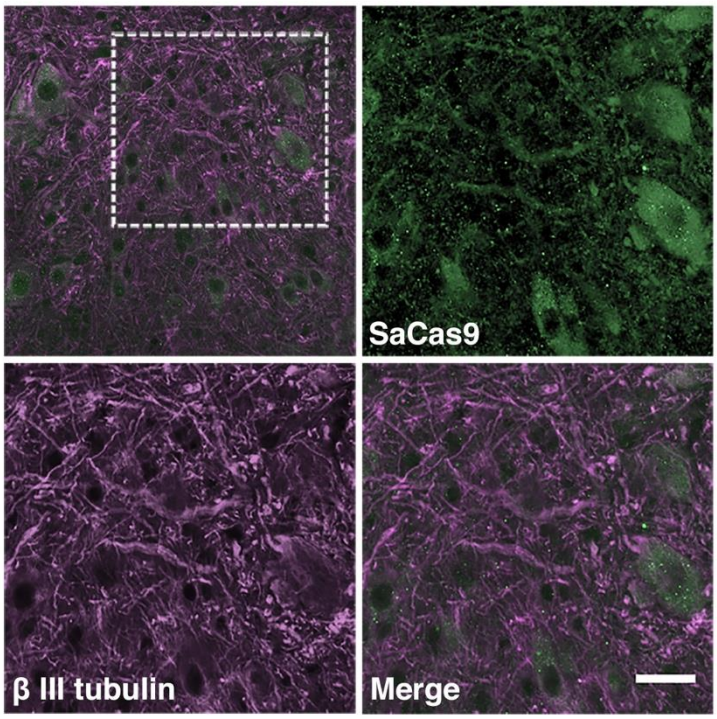

fig. S6. Systemic administration of AAV9-SaCas9-hSOD1 to neonatal G93A-SOD1 mice leads to SaCas9 expression in β3-tubulin^{+} fibers in the spinal cord. Immunofluorescent staining of thoracic spinal cord sections four weeks after G93A-SOD1 mice were injected with AAV9-SaCas9-hSOD1 (*n* = 3) or AAV9-SaCas9-mRosa26 (*n* = 3) via facial vein at P0-P1. Insets show high-magnification images. Scale bar, 25 μm.

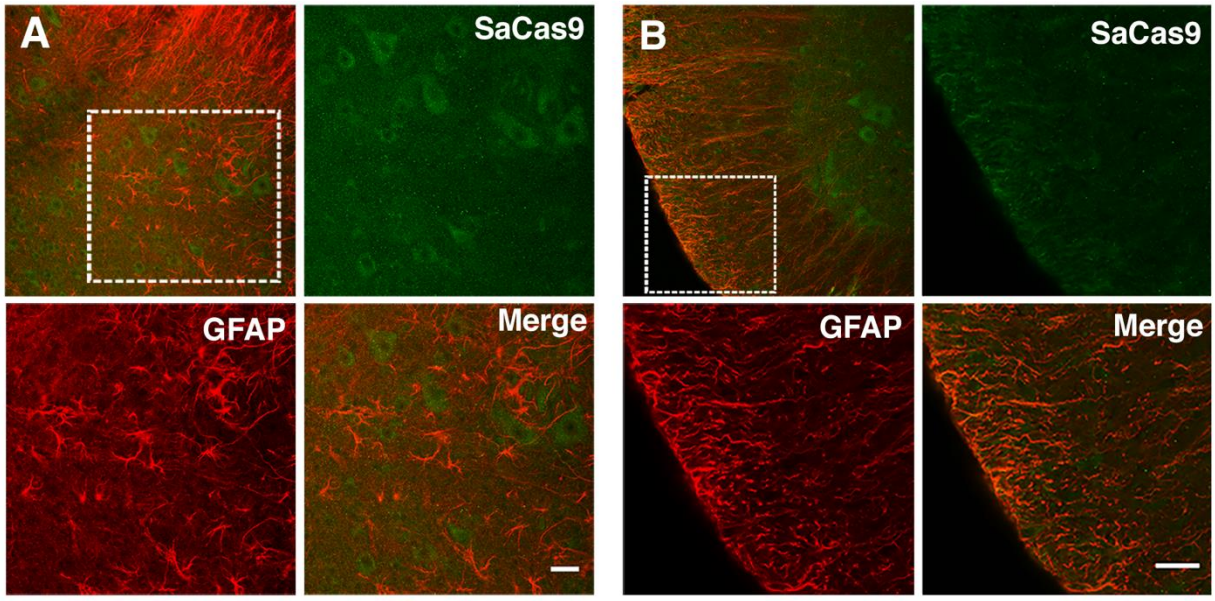

fig. S7. Systemic administration of AAV9-SaCas9-hSOD1 to neonatal G93A-SOD1 mice leads to limited SaCas9 expression in GFAP$^+$ astrocytes in the spinal cord.

Immunofluorescent staining of the **(A)** anterior grey column and **(B)** white matter four weeks after G93A-SOD1 mice were injected with AAV9-SaCas9-hSOD1 (*n* = 3) or AAV9-SaCas9-mRosa26 (*n* = 3) via facial vein at P0-P1. Insets show high-magnification images. Scale bar, 25 μm.

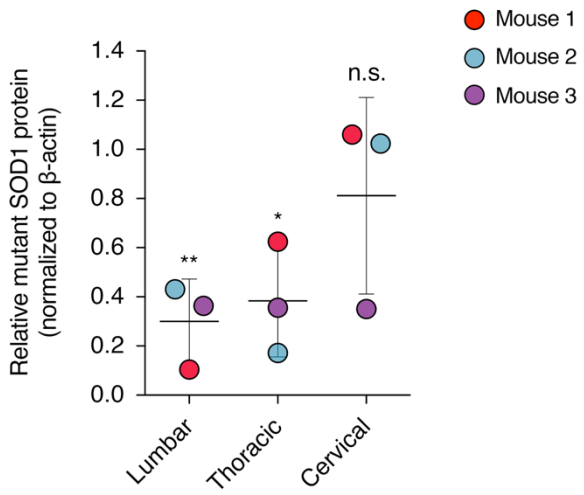

fig. S8. CRISPR-Cas9–mediated genome editing reduced mutant SOD1 protein in G93A-SOD1 mice. Quantitation of mutant SOD1 protein by western blot of lumbar, thoracic and cervical spinal cord lysate from G93A-SOD1 mice injected with AAV9-SaCas9-hSOD1 via facial vein (n = 3). Circles represent one of three individual mice. Mutant SOD1 protein in each lane was normalized to β-actin and compared to SOD1 protein from either the lumbar, thoracic or cervical spinal cord lysate of G93A-SOD1 mice injected with AAV9-SaCas9-mRosa26 (n = 3). Mean SOD1 protein values are indicated by the horizontal lines, and error bars represent S.D. **P = 0.001; *P < 0.05; n.s. indicates P > 0.05; two-way paired t-test.

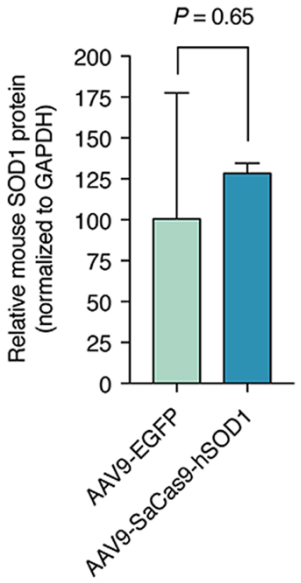

fig. S9. Genome editing did not affect mouse SOD1 protein in G93A-SOD1 mice. Western blot quantitation of native mouse SOD1 protein in whole spinal cord lysate four weeks after G93A-SOD1 mice were injected with AAV9-SaCas9-hSOD1 and AAV9-EGFP via facial vein at P0-P1. Mouse SOD1 protein was normalized to GAPDH in each lane. Values are means of three independent replicates, and error bars represent S.D. *P*-value calculated by two-way t-test.

A

B

	AAV9-SaCas9-hSOD1	AAV9-EGFP	P-value
mSOD1	0.013% ± 0.003%	0.011% ± 0.002%	0.391
OT1	0.020% ± 0.004%	0.014% ± 0.002%	0.158
OT2	0.018% ± 0.005%	0.013% ± 0.003%	0.432
OT3	0.018% ± 0.004%	0.017% ± 0.003%	0.746
OT4	0.008% ± 0.003%	0.008% ± 0.002%	0.866
OT5	0.033% ± 0.006%	0.034% ± 0.006%	0.848
OT6	1.164% ± 0.091%	1.316% ± 0.111%	0.141
OT7	0.022% ± 0.004%	0.017% ± 0.003%	0.159
OT8	0.022% ± 0.004%	0.019% ± 0.002%	0.357
OT9	0.009% ± 0.005%	0.007% ± 0.001%	0.725
OT10	0.018% ± 0.005%	0.019% ± 0.004%	0.939
OT11	0.016% ± 0.004%	0.051% ± 0.108%	0.696
OT12	0.018% ± 0.003%	0.024% ± 0.011%	0.478

fig. S10. Background modification at candidate OT sites in CRISPR-treated G93A-SOD1 mice. (A) Sequence and chromosomal location of potential OT sites identified by Cas-OFFinder. Mismatches from the on-target site in hSOD1 are colored pink. **(B)** Indel frequencies at candidate OT sites were measured by deep sequencing. Indels were measured within a 5 bp window around the predicted SaCas9 cleavage site in each OT site using CRISPResso. Frequencies are means from three independent replicates, and error bars indicate S.D. *P*-values calculated using two-tailed *t*-test.

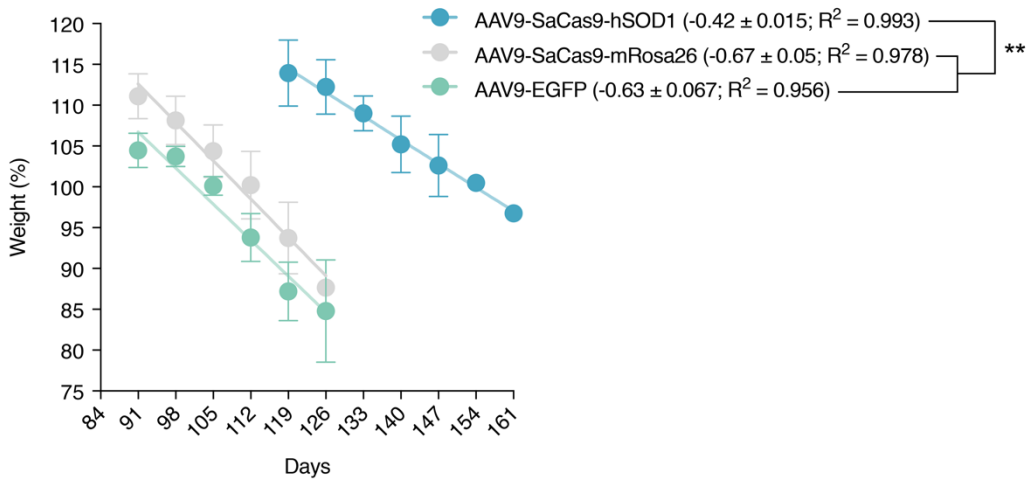

fig. S11. G93A-SOD1 mice treated with AAV9-SaCas9-hSOD1 lose weight at a slower rate after disease onset compared to control mice. Linear regression analysis of post-disease onset weights of G93A-SOD1 mice injected with AAV9-SaCas9-hSOD1 (n = 7), AAV9-SaCas9-mRosa26 (n = 7) or AAV9-EGFP (n = 7) via facial vein at P0-P1. Mean weights were normalized to the average 56-day values for each group. Values are means and error bars indicate S.E.M. Solid lines show the linear regression fit within each group. The slope values reported in the legend indicate weight loss (%) per day. Linear regression analysis was performed using Prism 7. $^{**}P < 0.005$.

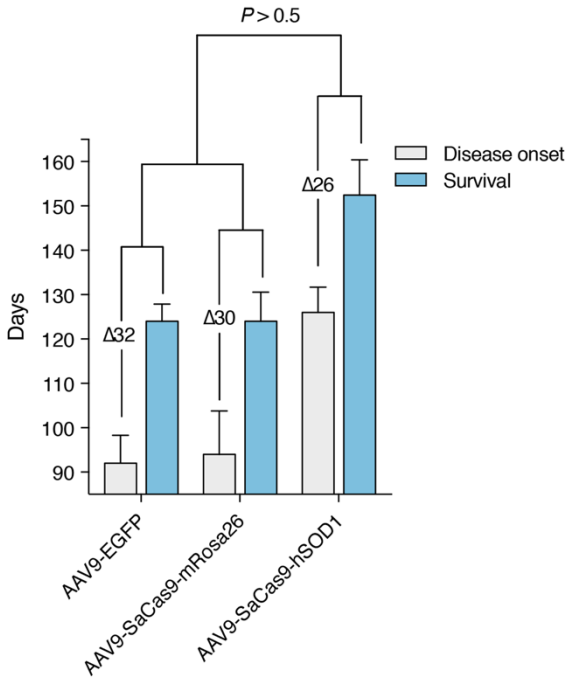

fig. S12. Systemic administration of AAV9-SaCas9-hSOD1 to neonatal G93A-SOD1 mice did not delay the rate of disease progression. Length of time from disease onset to death (Δ) in G93A-SOD1 mice injected with AAV9-SaCas9-hSOD1 (*n* = 7), AAV9-SaCas9-mRosa26 (*n* = 7) or AAV9-EGFP (*n* = 7) via the facial vein at P0-P1. Values are means and error bars indicate S.E.M. *P*-values calculated by one-way ANOVA followed by Tukey's post-hoc analysis.

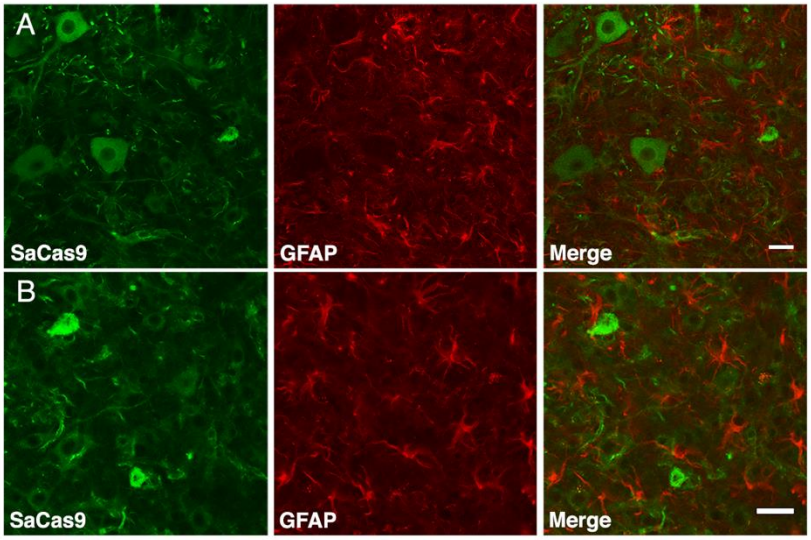

fig. S13. G93A-SOD1 mice injected with AAV9-SaCas9-SaCas9 had limited SaCas9 expression in GFAP$^+$ astrocytes at end stage. Immunofluorescent staining of end-stage spinal cord sections after G93A-SOD1 mice were injected with AAV9-SaCas9-hSOD1 via the facial vein at P0-P1. Scale bar, 25 μm.

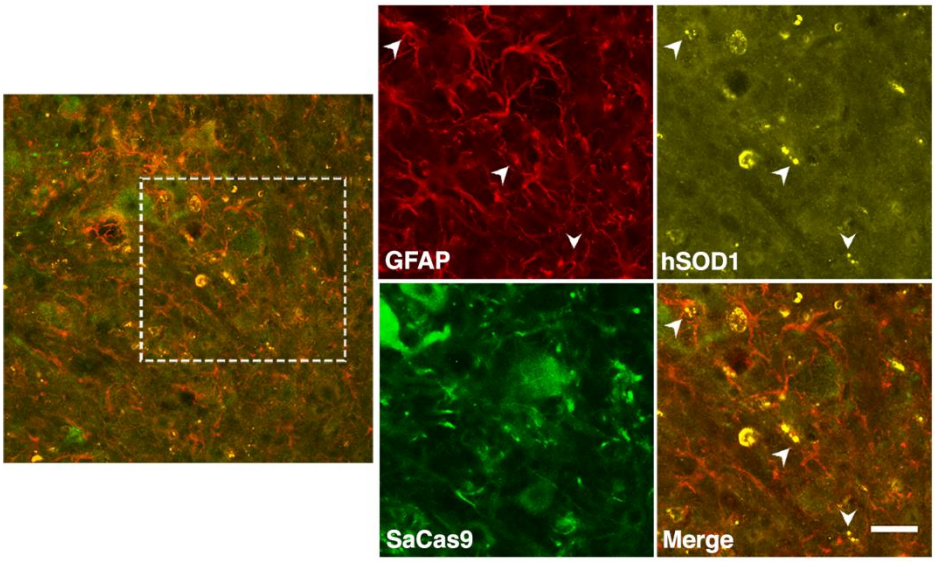

fig. S14. Mutant SOD1 inclusion bodies were visible in end-stage spinal cord sections from CRISPR-treated G93A-SOD1 mice. Immunofluorescent staining of end-stage spinal cord sections after G93A-SOD1 mice were injected with AAV9-SaCas9-hSOD1 via the facial vein at P0-P1. Arrowheads indicate GFAP$^+$ cells with immunoreactive mutant SOD1 inclusion bodies. Insets show high-magnification images. Scale bar, 25 μm.

table S1. Oligonucleotides used in this study.

Name	Sequence (5’ to 3’)
hSOD1 sgRNA 1 Fwd	CACCGCCTGCATGGATTCCATGTTC
hSOD1 sgRNA 1 Rev	AAACGAACATGGAATCCATGCAGGC
hSOD1 sgRNA 2 Fwd	CACCGGCCTGCATGGATTCCATGTTC
hSOD1 sgRNA 2 Rev	AAACGAACATGGAATCCATGCAGGCC
hSOD1 sgRNA 3 Fwd	CACCGAAGGCCTGCATGGATTCCATGTTC
hSOD1 sgRNA 3 Rev	AAACGAACATGGAATCCATGCAGGCCTTC
hSOD1 sgRNA 4 Fwd	CACCGCCGTCGCCCTTCAGCACGCACA
hSOD1 sgRNA 4 Rev	AAACTGTGCGTGCTGAAGGGCGACGGC
hSOD1 sgRNA 5 Fwd	CACCGCAGGCCTTCAGTCAGTCCTTTA
hSOD1 sgRNA 5 Rev	AAACTAAAGGACTGACTGAAGGCCTGC
hSOD1 sgRNA 6 Fwd	CACCGCCCACCGTGTTTTCTGGATA
hSOD1 sgRNA 6 Rev	AAACTATCCAGAAAACACGGTGGGC
pcDNA-hSOD1 Fwd	ACTCACGGGGATTTCCAAGTCTCCA
BGH-Rev	TAGAAGGCACAGTCGAGG
CMV-Fwd	CGCAAATGGGCGGTAGGCGTG
pcDNA-hSOD1-Rev	GCAATGGTCTCCTGAGAGTGAGATC
hSOD1-EcoRI-Fwd	TGGTACCGAGCTCGGATCCACTAGT
qPCR-CMV-Fwd	ATGGTGATGCGGTTTTGGCAG
qPCR-CMV-Rev	GGCGGAGTTGTTACGACATTTTGG
hSOD1-Tg-Fwd	GGAGGTTCACTGGCTAGAAAGTGGTCA
hSOD1-Tg-Rev	AGCGACAGAGCAAGACCCTTTCTC

table S2. External primers for MiSeq analysis.

Name	Sequence (5’ to 3’)	Off target (OT) site
1-EXT_F	AGCTACCCTGTTTCCGGGTTTAT	OT1: chr8:78319778
1-EXT_R	CCACGGAGGGGTTTGTTGATTG	OT1: chr8:78319778
2-EXT_F	TGCCATTGGATCCCTTTTCCCT	OT2: chr7:81747567
2-EXT_R	CACTCGCTCTGGCTCATAGGTT	OT2: chr7:81747567
3-EXT_F	GAGTCCTTCCCACTGCTCCAAT	OT3: chr4:139152867
3-EXT_R	GTACACAGACACACATGCAGGC	OT3: chr4:139152867
4-EXT_F	GGCTCTGTGTGGGAGAGTTGAT	OT4: chr5:72856043
4-EXT_R	TTTGGGTCCCATCACGCTGTAT	OT4: chr5:72856043
5-EXT_F	CCATTTGCCTTCCCTGCCTTTT	OT5: chr16:18970882
5-EXT_R	CTCCACTTACAGGCTGGCTCTT	OT5: chr16:18970882
6-EXT_F	GGCCACTATGTGAACACAGTGC	OT6: chr1:166902806
6-EXT_R	CACCCCAACCCTTCCCATAACT	OT6: chr1:166902806
7-EXT_F	TCAGTGTTCCCATGGCTAACGT	OT7: chr15:41362712
7-EXT_R	TGGTGGAATTTTTGGCGTCACT	OT7: chr15:41362712
8-EXT_F	CTGTAATGGGATCCGATGCCCT	OT8: chr10:62443153

8-EXT_R	ATTCCACTCAGGCCCTACCAAC	OT8: chr10:62443153
9-EXT_F	TGCTCATGACACACCAACCTCA	OT9: chr6:34213859
9-EXT_R	TGGTTTGCTCAGCCTACTCTCC	OT9: chr6:34213859
10-EXT_F	AGTTAGAGGTGGCTGTGAGCTG	OT10: chr6:95468813
10-EXT_R	AGTGGATACGTTTGCCTTCCGA	OT10: chr6:95468813
11-EXT_F	CTTGCATGCCCCAAATGTGACT	OT11: chr9:75741573
11-EXT_R	AAACGAGAACGGGTGGTACTACA	OT11: chr9:75741573
12-EXT_F	CCTCCTGAAGGTCTTTCCCTGG	OT12: chr11:69006483
12-EXT_R	GCTGGAGAGATGGTTCAGTGGT	OT12: chr11:69006483
13-EXT_F	GGAGGTTCACTGGCTAGAAAGTGGTCA	hSOD1
13-EXT_R	AGCGACAGAGCAAGACCCTTTCTC	hSOD1
14-EXT_F	GCATCTGGCAGCAAGTGTTAGG	mSOD1: chr16:90220754-90224140
14-EXT_R	TGTGGAGAAGGGAAGAAGGCAG	mSOD1: chr16:90220754-90224140

table S3. Internal primers for MiSeq analysis. Barcodes underlined.

Name	Sequence (5’ to 3’)
1-INT_F	AATGATACGGCGACCACCGAGATCTACACTCTTTCCCTACACGACGCTCTTCCGATCTATGTTATAGCCAAAGATTAATTTCTCTTTGCTTGAGA
1-INT_R	CAAGCAGAAGACGGCATACGAGATGCCTAAGTGACTGGAGTTCAGACGTGTGCTCTTCCGATCTAATGTTTCTGGCGGTCTTTTTTTTTTTCCCCGTG
2-INT_F	AATGATACGGCGACCACCGAGATCTACACTCTTTCCCTACACGACGCTCTTCCGATCTCTCTCTTGTCAGATGGCTCCCCAC
2-INT_R	CAAGCAGAAGACGGCATACGAGATCTGATCGTGACTGGAGTTCAGACGTGTGCTCTTCCGATCTTCTTAGTTAATGGCATTAAATACTTTTATTTTTATT
3-INT_F	AATGATACGGCGACCACCGAGATCTACACTCTTTCCCTACACGACGCTCTTCCGATCTGACTGGTTATGTTGATATATGATCTGTAGTGAATCTTTC
3-INT_R	CAAGCAGAAGACGGCATACGAGATAAGCTAGTGACTGGAGTTCAGACGTGTGCTCTTCCGATCTTCTGTGTCACCACTTGTTTTTGGTG
4-INT_F	AATGATACGGCGACCACCGAGATCTACACTCTTTCCCTACACGACGCTCTTCCGATCTTCGAAGTGGGGCTGAGAACCAGG
4-INT_R	CAAGCAGAAGACGGCATACGAGATGTAGCCGTGACTGGAGTTCAGACGTGTGCTCTTCCGATCTTTCTTCATAGACACTGGGGAATTACC
5-INT_F	AATGATACGGCGACCACCGAGATCTACACTCTTTCCCTACACGACGCTCTTCCGATCTATCGCCTGAGAGCACACACTGCCCCT
5-INT_R	CAAGCAGAAGACGGCATACGAGATTTGACTGTGACTGGAGTTCAGACGTGTGCTCTTCCGATCTTAGGAATGAGGCCTAAGAAAAAGAGTGAG
6-INT_F	AATGATACGGCGACCACCGAGATCTACACTCTTTCCCTACACGACGCTCTTCCGATCTGTCAGACCCCCAGTTAATTCTGATTGGTATTGGAA
6-INT_R	CAAGCAGAAGACGGCATACGAGATTGACATGTGACTGGAGTTCAGACGTGTGCTCTTCCGATCTCCTGGCACATGGCTACTACCT

7-INT_F	AATGATACGGCGACCACCGAGATCTACACTCTTTCCCTACACGACGCT CTTCCGATCTTGCATCGAAACATTGGTGACCTGAAACTTCCTATGT
7-INT_R	CAAGCAGAAGACGGCATACGAGATCTCTACGTGACTGGAGTTCAGAC GTGTGCTCTTCCGATCTCTGAGACATAAGAAAACTTACATTAAAAAAA TACAT
8-INT_F	AATGATACGGCGACCACCGAGATCTACACTCTTTCCCTACACGACGCT CTTCCGATCTCTACGTGATAGGTCTTGTTTTCACCCCTGA
8-INT_R	CAAGCAGAAGACGGCATACGAGATGCGGACGTGACTGGAGTTCAGAC GTGTGCTCTTCCGATCTGAGGTGATGGCACTGACATG
9-INT_F	AATGATACGGCGACCACCGAGATCTACACTCTTTCCCTACACGACGCT CTTCCGATCTACTCGTGATTAGGATGCTCAGAGTTTTCTGTGA
9-INT_R	CAAGCAGAAGACGGCATACGAGATTTTCACGTGACTGGAGTTCAGAC GTGTGCTCTTCCGATCTCTATTCAAGGCACAGAGTGGG
10-INT_F	AATGATACGGCGACCACCGAGATCTACACTCTTTCCCTACACGACGCT CTTCCGATCTACATGACATATGCCTTAACAATGAAGAAGC
10-INT_R	CAAGCAGAAGACGGCATACGAGATGGCCACGTGACTGGAGTTCAGAC GTGTGCTCTTCCGATCTCTATTACAGATGGAAGTCACTTGGG
11-INT_F	AATGATACGGCGACCACCGAGATCTACACTCTTTCCCTACACGACGCT CTTCCGATCTCTTTAAGAGCATAGAAGGAGTGGCT
11-INT_R	CAAGCAGAAGACGGCATACGAGATCGAAACGTGACTGGAGTTCAGAC GTGTGCTCTTCCGATCTGAAAACTTTATAACTACTGTGTGTTAACAGA C
12-INT_F	AATGATACGGCGACCACCGAGATCTACACTCTTTCCCTACACGACGCT CTTCCGATCTGACCCCGGGCTGGTTTGATTCCCA
12-INT_R	CAAGCAGAAGACGGCATACGAGATCGTACGGTGACTGGAGTTCAGAC GTGTGCTCTTCCGATCTATAAGTCTTGGCTGGTCTCAAACTCACTGTG
13-INT_F	AATGATACGGCGACCACCGAGATCTACACTCTTTCCCTACACGACGCT CTTCCGATCTAACTTTTCTTAAAGGAAAGTAATGGACCAGTGAAGG

13-INT_R	CAAGCAGAAGACGGCATACGAGATTGCCGAGTGACTGGAGTTCAGAC GTGTGCTCTTCCGATCTGGTGAACAAGTATGGGTCACCAGCAC
14-INT_F	AATGATACGGCGACCACCGAGATCTACACTCTTTCCCTACACGACGCT CTTCCGATCTATCGCTTTTAAATCAAGGCAAGCGGTGAAC
14-INT_R	CAAGCAGAAGACGGCATACGAGATGCTACCGTGACTGGAGTTCAGAC GTGTGCTCTTCCGATCTGTTCCTTTCCATCACTGGTCACTAGCC